

Earth Surface Dynamics Discussion

Supplementary Information for

Comparison of calibration characteristics of different acoustic impact systems for measuring bedload transport in mountain streams

Dieter Rickenmann¹, Lorenz Ammann¹, Tobias Nicollier¹, Stefan Boss¹, Bruno Fritschi¹, Gilles Antoniazza^{2,1}, Nicolas Steeb¹, Zheng Chen^{1,3,4}, Carlos Wyss^{1,5}, Alexandre Badoux¹

¹Swiss Federal Research Institute WSL, Birmensdorf, 8903, Switzerland

²Institute of Earth Surface Dynamics (IDYST), University of Lausanne, Lausanne, 1015, Switzerland

³Institute of Mountain Hazards and Environment, Chinese Academy of Sciences, Chengdu, 610041, China

⁴University of Chinese Academy of Sciences, Beijing, 100049, China

⁵wyss.io - Dr. Carlos R. Wyss Engineering, Zürich, 8052, Switzerland

Contents of this file

Figures S1 to S15

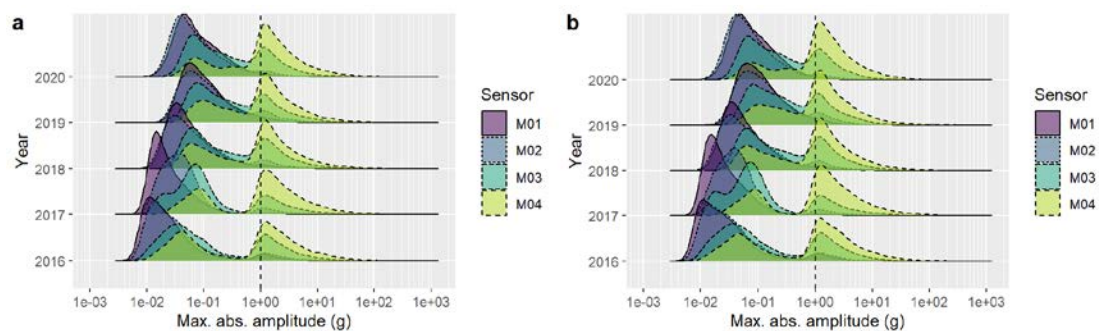


Figure S1: Erlenbach site. Maximum amplitude of each sensor for all packets by year. (The thresholds used for packet identification is indicated by the dashed line.) (a) Determined from the original data with a sampling rate of 20 kHz, (b) determined from the data down-sampled to 10 kHz.

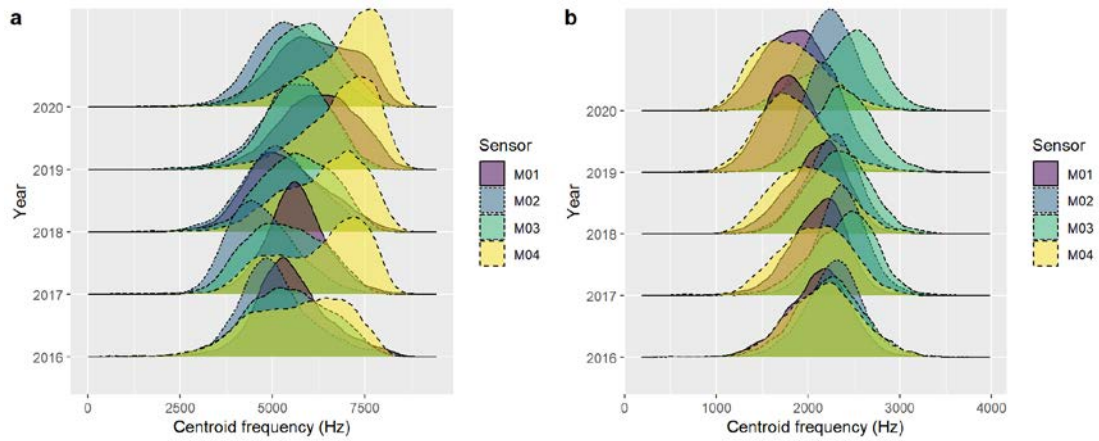


Figure S2: Erlenbach site. Centroid frequency of all packets by year. (a) Determined from the original data with a sampling rate of 20 kHz, (b) determined from the data down-sampled to 10 kHz.

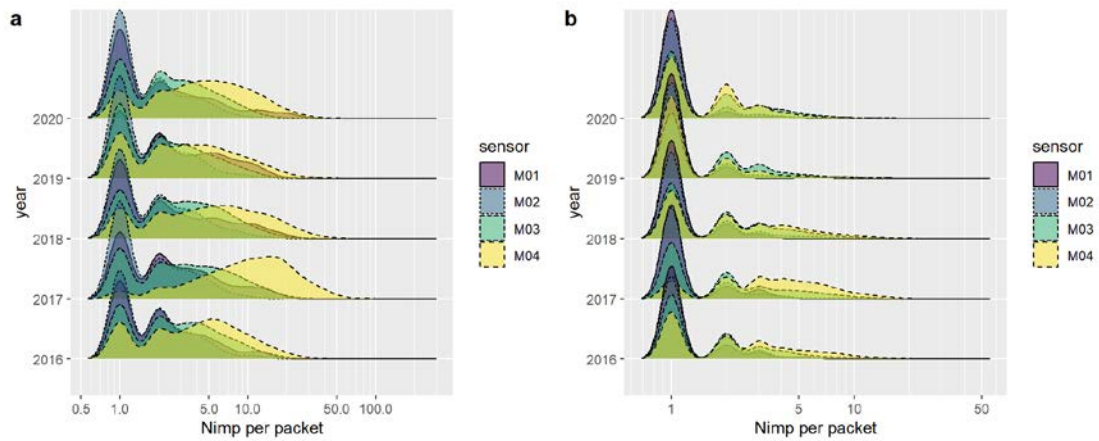
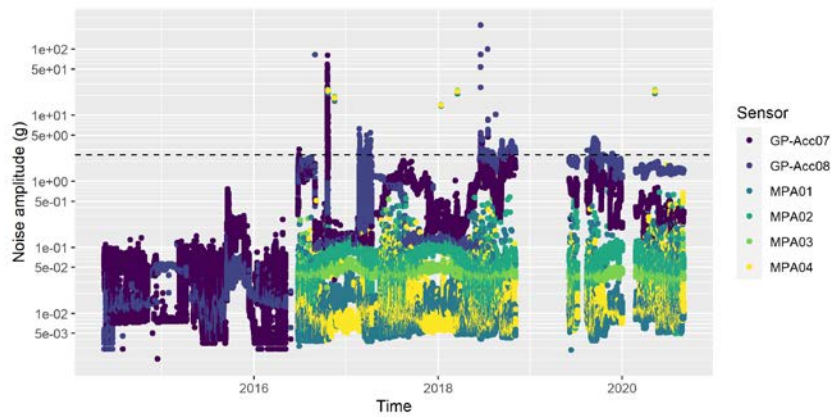
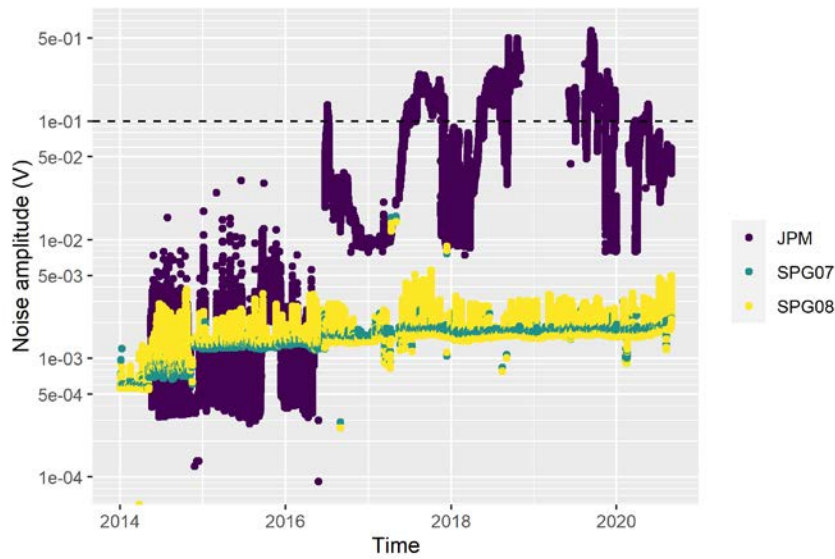


Figure S3: Erlenbach site. Combined no. of impulses (Nimp) of each sensor per packet by year. (a) Determined from the original data with a sampling rate of 20 kHz, (b) determined from the data down-sampled to 10 kHz. Transport intensities generally increase laterally in the measuring cross-section from the orographic left to right (in flow direction), implying that plate M04 observes higher transport intensities than plate M01.



(a)



(b)

Figure S4: Background noise evolution over time. (a) MPA and GP-Acc at the Erlenbach. Accelerometer measurements before 20.06.2016 have been converted from V to g by multiplication with the conversion coefficient 50 g/V. (b) SPG and JPM at the Erlenbach.

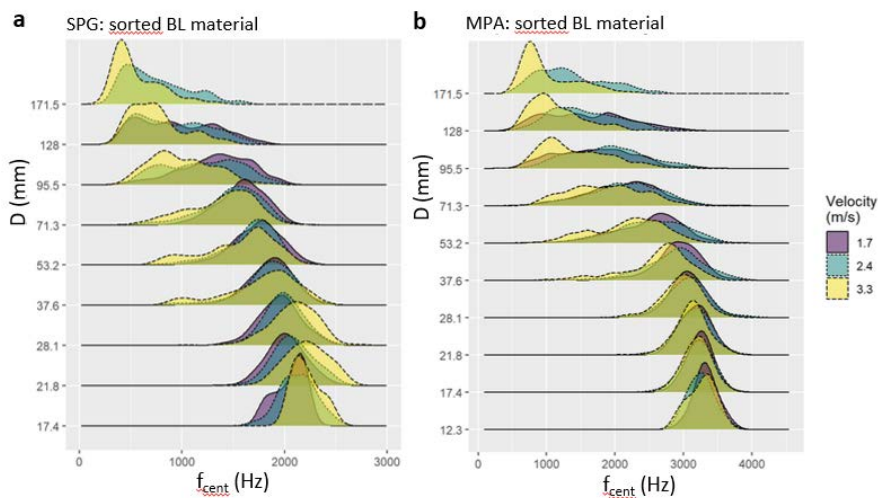
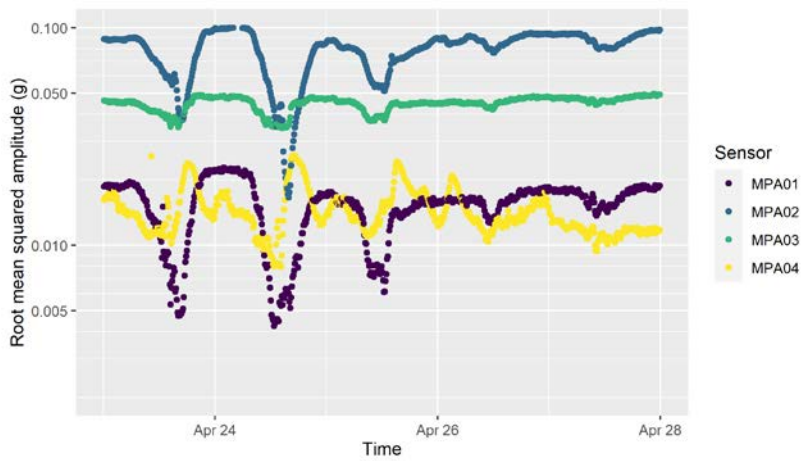
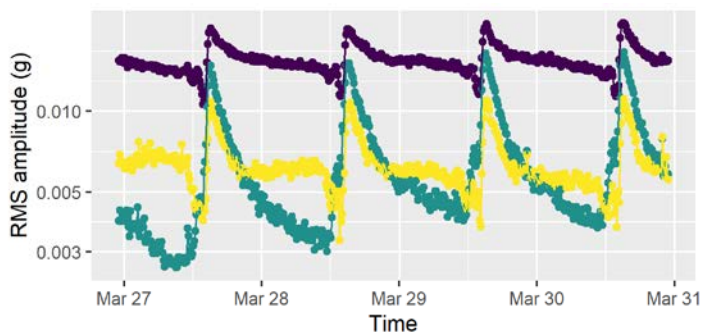


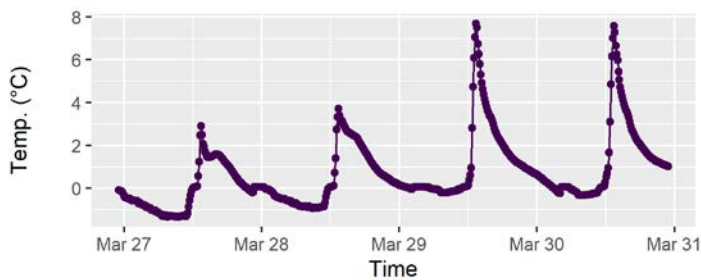
Figure S5: Obernach flume site. Grain size (class) D vs. centroid frequency f_{cent} recorded for packets with the 5 largest amplitudes per experimental run. Velocity is the water velocity 10 cm above the impact plates. (a) for the SPG system (packets for $A > 0.03V$), and (b) for the MPA system (packets for $A > 0.69g$)



(a)



(b)



(c)

Figure S6: Daily cycles of the MPA noise level (i.e. root mean square RMS of amplitude) at (a) Erlenbach in April 2017 and (b) Avançon in March 2019, and (c) of water temperature in the Avançon stream in March 2019.

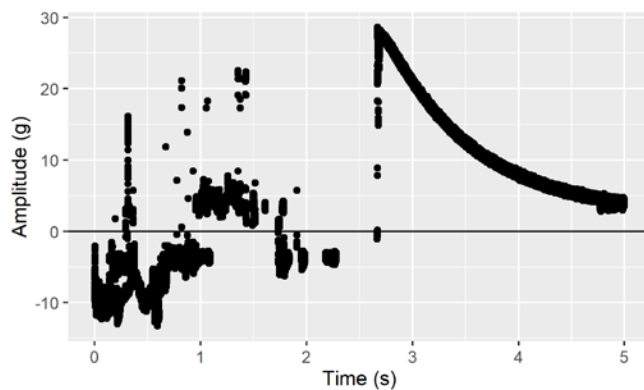


Figure S7: Unstable signal recorded with GP-Acc at the Erlenbach site, shown as signal amplitude vs. time. This is a rather typical behavior of this sensor type at the Erlenbach. A signal saturation is visible at a time of approximately 2.6 seconds, lasting about 2 seconds.

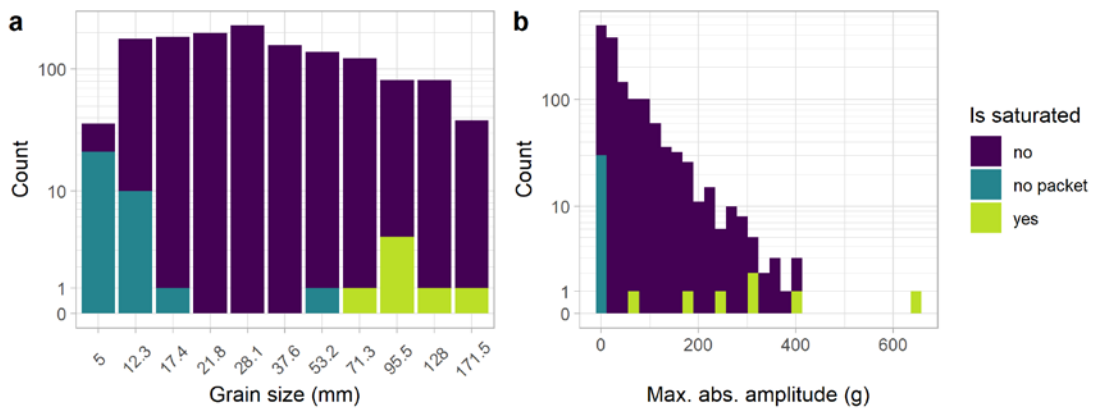


Figure S8: Signal saturation of MPA signal for each experiment at Obernach. The count of experiments is shown (a) as a function of the grain size (of the single grain size class experiments) and (b) the maximal amplitude recorded. For each experiment, the color indicates whether a signal saturation was determined, or whether no packet was recorded at all. (Note distortions due to log-scale in both panels)

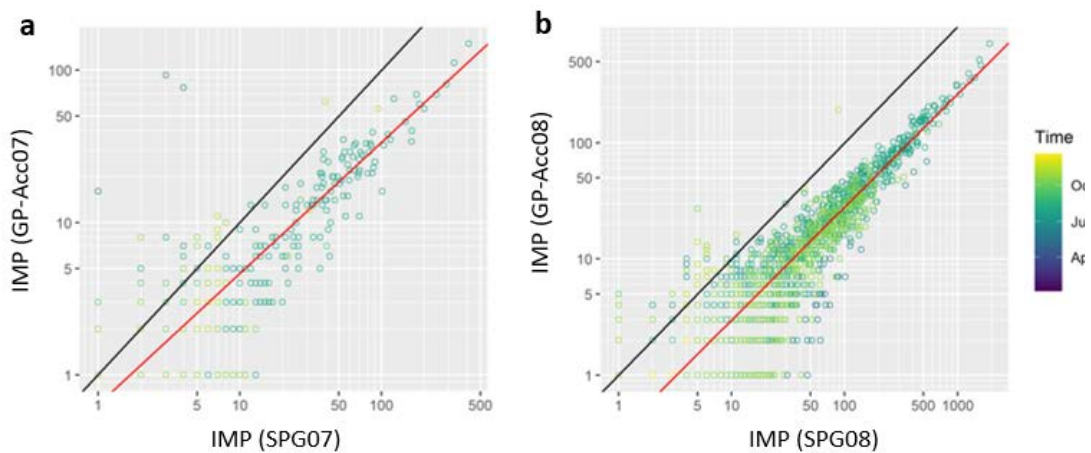


Figure S9: Erlenbach field site. Number of impulses IMP registered per minute with sensor GP-Acc vs. sensors GP-Geo (SPG), showing data for the year 2014 only. (a) Impacts on plate 07, on the left (in flow direction) of the channel center line, with generally weaker bedload transport; (b) Impacts on plate 08, on the right of the channel center line, with generally stronger bedload transport. All the time steps for which either of the two sensors registered zero impulses were removed for plotting. Black line: 1:1-line, red line: power-law regression. For the fit of the power-law, only $IMP (SPG) > 50$ and $IMP (GP-Acc) > 10$ were used.

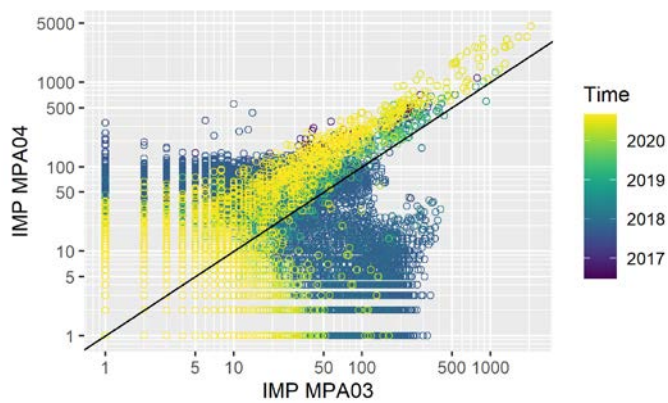


Figure S10: Erlenbach field site. Number of impulses registered per minute with sensor MPA04 vs. sensor MPA03. All the time steps for which either of the two sensors registered zero impulses were removed for plotting. Both MPA plates 03 and 04 are on the right of the channel center line (in flow direction), and there is generally stronger bedload transport over plate 04 than over plate 03.

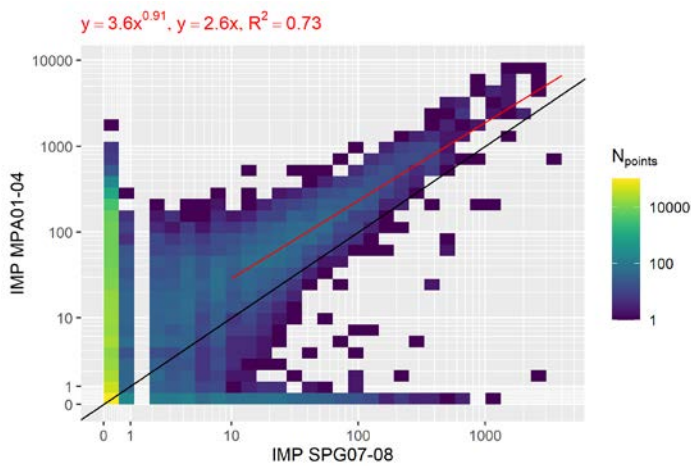


Figure S11: Erlenbach field site. SPG and MPA impulses during each one-minute time-step. Time-steps for which either of the sensor types registered zero impulses are plotted at the edge of the panel, time-steps for which either of the two sensor types recorded less than 10 impulses were excluded for calculating the regression. The blue to yellow colors indicate the density of the data points.

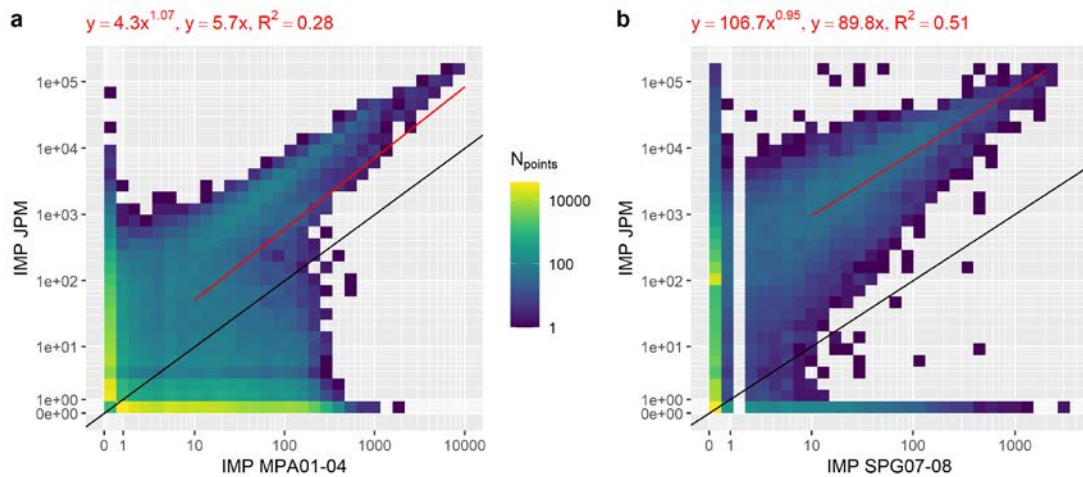


Figure S12: Erlenbach field site. JPM impulses during each 1-minute timestep at the Erlenbach compared to (a) MPA and (b) SPG impulses. Timesteps for which either of the sensor types registered 0 impulses are plotted at the edge of the panel, time-steps for which either of the two sensor types recorded less than 10 impulses were excluded for calculating the regression. The blue to yellow colors indicate the density of the data points.

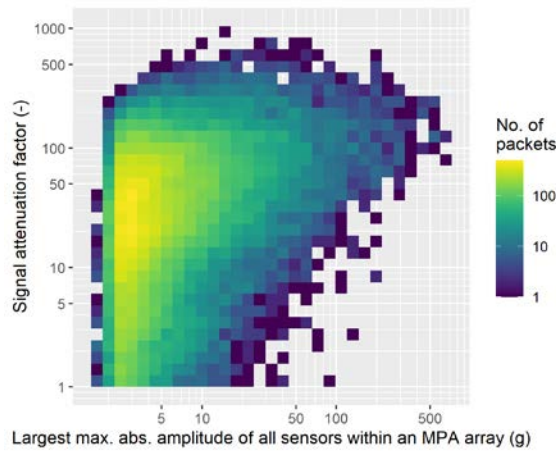


Figure S13: Avançon de Nant field site. Lateral signal attenuation estimated for the MPA. For all packets recorded during the calibration experiments, the signal attenuation factor (y-axis) was calculated as the ratio of the largest divided by the second largest maximal abs. amplitude among all 4 accelerometers of one MPA array covering a stream width of 1 m. Here the multidimensional packet approach was used, whereby the signal from adjacent sensors is analyzed jointly as one packet. The blue to yellow colors indicate the density of the packets.

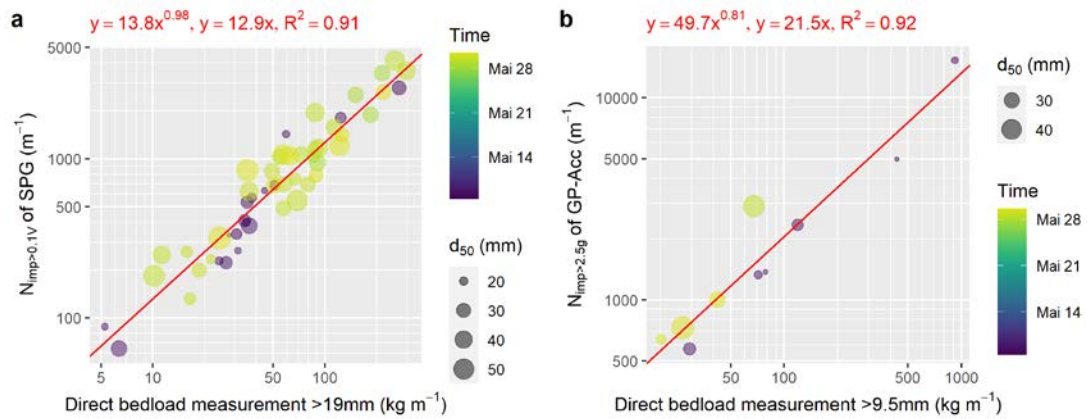


Figure S14: Albula field site. Calibration relation in terms of number of impulses IMP vs. bedload mass M . (a) SPG impulses and (b) GP-Acc impulses plotted vs. direct bedload measurements. One GP-Acc calibration experiment was removed for this plot due to implausible signal presumably caused by sensor malfunctioning.

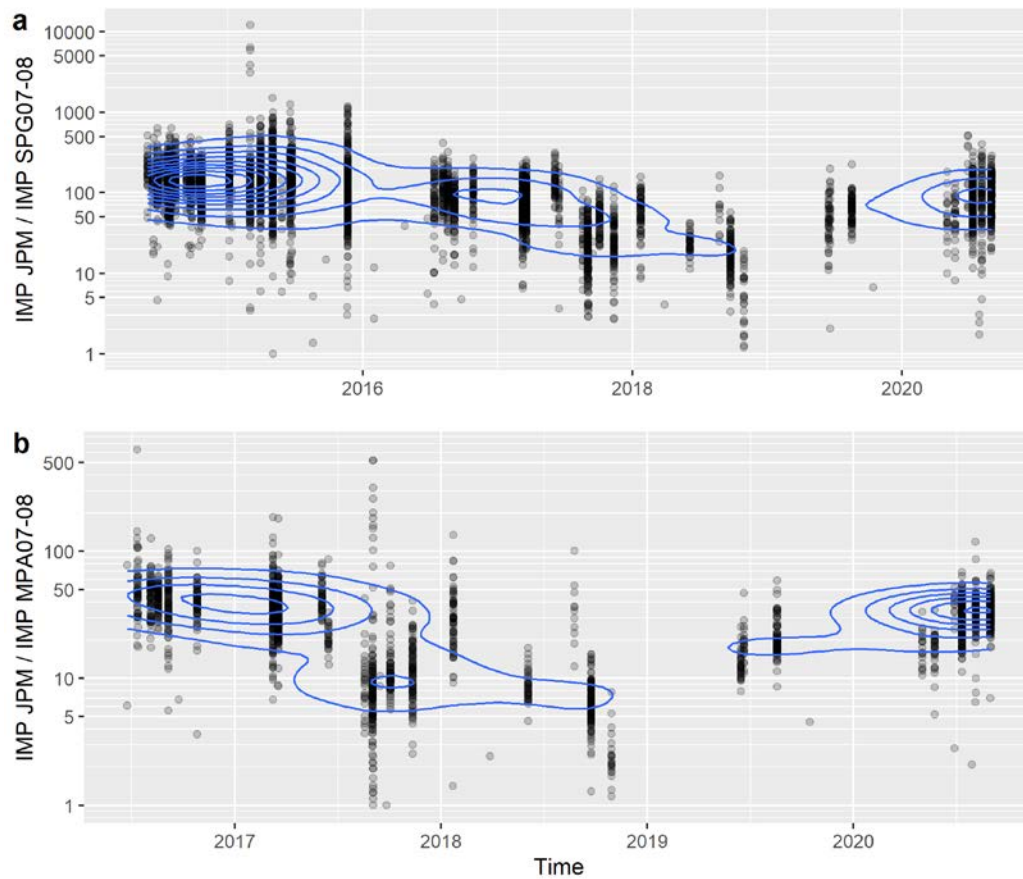


Figure S15: Erlenbach field site. Ratio of impulses of JPM to (a) SPG and (b) MPA per minute over multiple years. Time-steps with less than 10 GP impulses were removed for this plot.